

The influence of charge-mode operation of a XeCl laser on the beam profile

F.A. van Goor^a, J.C.M. Timmermans^b, W.J. Witteman^a

^a University of Twente, Department of Applied Physics, P.O. Box 217, 7500 AE Enschede, The Netherlands

^b Nederlands Centrum voor Laser Research (NCLR) b.v., P.O. Box 2662, 7500 CR Enschede, The Netherlands

Received 27 July 1995; revised version received 27 September 1995

Abstract

The shape of the beam profile of a discharge excited XeCl excimer laser using a spiker-sustainer electrical circuit has been varied from a 'bell'-, through a 'top-hat'-, to a 'camel-back'-profile by varying the delay between the spiker pulse and the main-current with the circuit operating in the charge-mode. Fine-tuning of the beam profile can be done by varying the charging voltage of the main pulse forming network or the temperature of a gas purifier regulating the Xe and HCl partial pressures.

1. Introduction

The shape of the beam profile of a XeCl laser is of increasing importance for many industrial applications. In most cases, where stable resonators are used, the beam of a XeCl laser is rectangular reflecting the transverse dimensions of the discharge. The laser intensity distribution has a more or less rectangular shape in the direction of the electric field of the discharge and some sort of a bell shape in the other transverse direction. The latter shape depends on factors like the contours of the discharge electrodes and the distribution of the pre-ionisation electron density prior to the breakdown of the discharge. A number of techniques are used to reshape the beam to the desired profile. These include optimisation of the contours of the discharge electrodes and the application of diffractive optics.

In this communication we describe a method to fine-tune the shape of the laser intensity profile during operation of the laser without the need of any additional optics. For this we intentionally postpone the start of the discharge in a high-pressure mixture of HCl, Xe

and Ne after application of a spiker-pulse initiating the breakdown [1]. During this delay the electron distribution in the direction transverse to the electrical field, just after completion of the electron avalanche, will change to the desired shape. The profile of the laser beam is determined by the power deposition profile given by $P = e n_e \mu(E/N) E^2$, where e is the electron charge, n_e the electron density, $\mu(E/N)$ the electron mobility, and E the electric field. Therefore the beam profile will depend on the spatial dependency of the electrical field and on the electron density distribution during the main discharge. The reshape of the spatial distribution of the electron density is caused by a spatial and time dependent loss of electrons by dissociative attachment to vibrational excited HCl [1–3]. Also a spatial dependent step-wise ionisation of Xe* could cause a spatial redistribution of electrons during the electron decay between the two discharges. The spatial distribution of the E/N is mainly determined by the shapes of the electrodes which was held constant during these experiments, so the beam profile depends essentially on the electron density profile.

2. Experimental configuration

The experiments have been performed with a XeCl laser system having a $3\text{ cm} \times 2\text{ cm} \times 80\text{ cm}$ (electrode distance \times width \times length) high pressure discharge pre-ionised by a 50 ns duration X-ray pulse. The mixture consisted of Xe, HCl and Ne at a total pressure of $5 \times 10^5\text{ Pa}$. The partial pressures of Xe and HCl could be varied with an Oxford Lasers gas purifier model GP2000 by adjusting the temperature of a condensing surface. Details of the construction of the laser head and the X-ray pre-ioniser have been published previously [4,5]. Although it can be expected that the experimental results described in this paper depend on the distribution of the electrical field in the discharge region and hence on the shape of the electrodes we did not vary the electrode structure in our laser. The electrodes

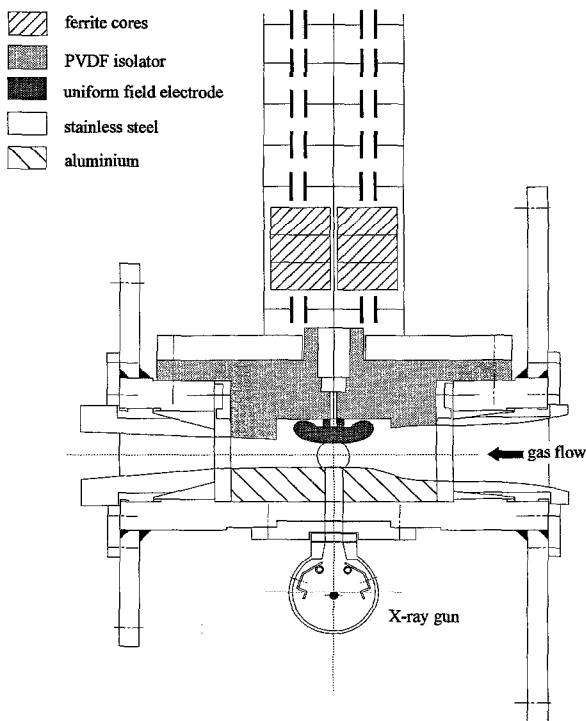


Fig. 1. Cross-section of the laser head. The laser is part of a wind-tunnel (not shown) to allow high repetition rate operation. A part of the electrical circuit, mounted on top of the laser head, is shown schematically. The 2.8 nF peaking capacitor is mounted as close to the discharge as possible and is distributed along the length of the laser. The 530 nF pulse forming network consists of ten rows of ceramic capacitors arranged in a double-plate configuration.

used were a nickel uniform field electrode embedded in a PVDF insulator and a flat aluminium electrode that was 1 mm thick in a 2 cm wide slit in order to transmit the X-ray pre-ionisation pulse. Fig. 1 shows the cross-section of the laser head. The laser head is part of a wind tunnel (not shown) to allow high-repetition rate operation of the laser [4]. The resonator consisted of a 10 m radius concave total reflector and a flat 50% reflecting outcoupling mirror separated 120 cm. The discharge was excited by a spiker-sustainer circuit using a 'race-track' saturable inductor as the low-inductance main switch. Fig. 2 shows the electrical circuit schematically. The laser could operate in the 'resonant overshoot mode' [6] and in the 'charge mode' [7]. The spiker circuit includes a one-step pulse compression circuit that has two functions: Firstly, it increases the rise time and duration of the current pulse through the spiker thyatron which helps to increase the life time of this thyatron at high repetition rate operation and secondly it plays an important role when the circuit operates in the charge mode. Typical wave forms of the voltage, current, and laser output are shown in Fig. 3 where the laser operates in the charge-mode. Fig. 4 shows wave forms for resonant overshoot operation. It can be seen from Fig. 3 that for charge-mode operation the discharge current starts a few tens of nanoseconds after the breakdown caused by the spiker pulse. This can be explained as follows [7,8]: The saturable inductors, L_p and L_c , are initially in the reversed saturated state caused by the PFN-charging current that still has a non-zero value. For charge mode operation it is essential that the spiker is fired a few hundred of nanoseconds

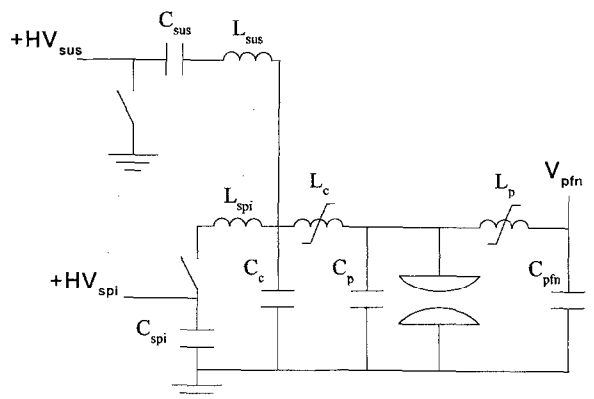


Fig. 2. Schematic of the spiker-sustainer circuit: $C_{sus} = 640\text{ nF}$, $C_{pfn} = 530\text{ nF}$, $C_p = 2.8\text{ nF}$, $C_c = 2.7\text{ nF}$, $C_{spi} = 5.4\text{ nF}$.

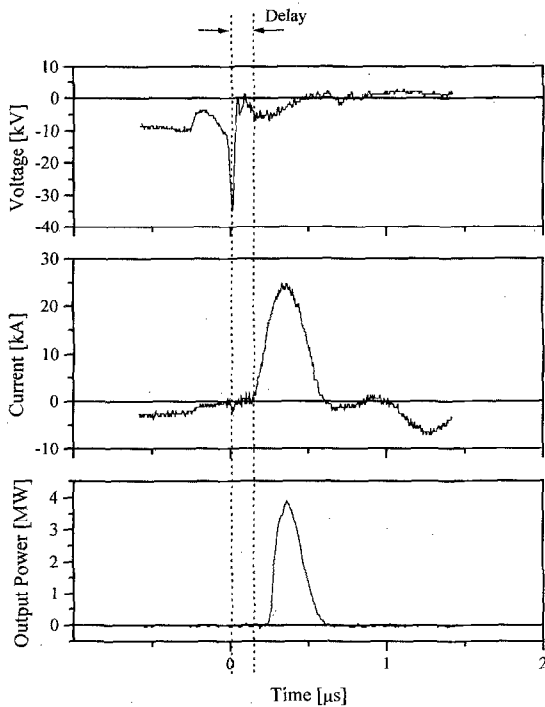


Fig. 3. Wave forms of the discharge voltage, current and laser output power for charge mode operation.

before the charging current of the PFN capacitor, C_{PFN} , crosses zero. When, after pre-ionisation, the spiker thyatron fires, the voltage on the capacitor C_c of the pulse compression circuit changes from a negative voltage, which is equal to the PFN charging voltage, to a positive value in about 100 ns. Because the PFN charging current is still flowing and L_c is brought into a high inductive state by the spiker circuit, effectively isolating C_c from the PFN, the voltage across C_c swings to a high negative voltage because of resonant charging of C_c . After this voltage swing, the inductor L_c saturates again and C_c is discharged into the peaking capacitor, C_p , resulting in the short rise-time, high negative voltage spike that is characteristic for the charge mode. It is essential for both the charge- and the resonant overshoot mode that the charging current of the PFN flows through the saturable inductors as indicated in Fig. 2. This results in a reset of the cores in the correct direction prior to the shot. After breakdown of the gas by the spiker pulse, the saturable inductor L_p , which acts as the main switch, must be brought into a low inductive state by saturation of the core in the forward direction

in order to discharge the PFN capacitor, C_{PFN} . When the circuit operates in the resonant overshoot mode the core is saturated in the correct direction when the PFN current starts to flow. (This is true when the breakdown voltage is lower than the maximum voltage that the spiker circuit can generate when the discharge has an infinite impedance (i.e. no pre-ionisation) [8]). In this case no delay occurs. In case of charge mode operation, however, the core has to be set into the forward direction after the spiker voltage pulse. This causes a delay of a few tens of nanoseconds. This delay depends on the voltage across the inductor L_p , which is almost equal to the PFN voltage, V_{PFN} , prior to the breakdown. Fig. 5 shows voltage- and current wave forms at several PFN charging voltages. Fig. 6 depicts the delay as a function of V_{PFN} . The laser generates an output energy of about 1 J at an efficiency of 2% for a charging voltage of about four times the DC-breakdown voltage (~ 4 kV) and 0.6 J at 3% efficiency for twice the DC-breakdown voltage where the pulse forming network impedance is matched to the discharge impedance (Fig. 7) and no current reversals appear as shown in Fig. 5. For resonant overshoot mode operation the efficiency and

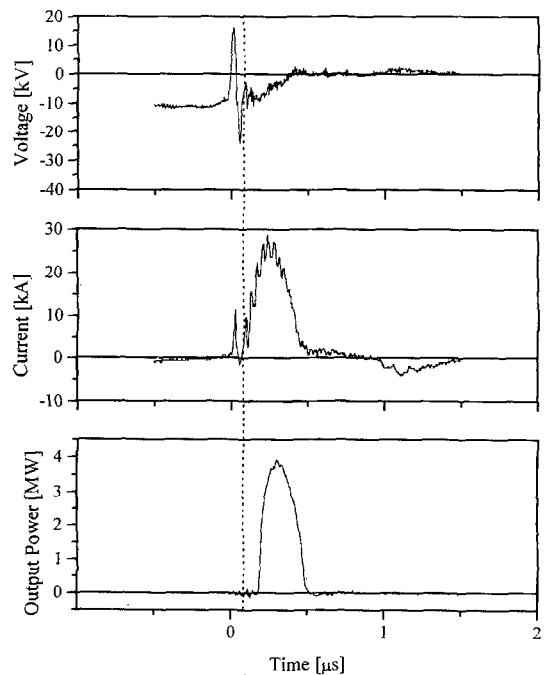


Fig. 4. Wave forms of the discharge voltage, current and laser output power for resonant overshoot mode operation.

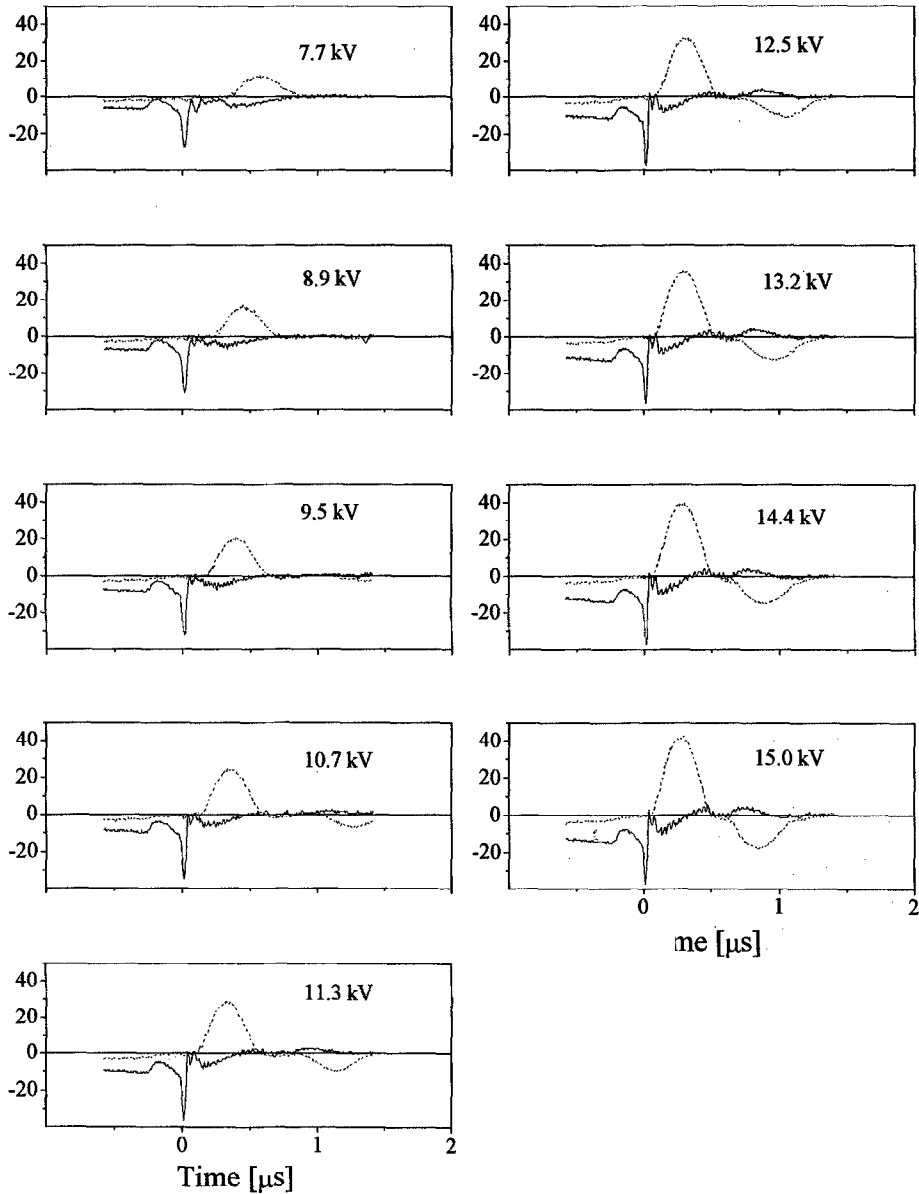


Fig. 5. Wave forms of the discharge voltage and current of the laser operating in the charge mode at several PFN charging voltages.

output energy are slightly higher, because with charge mode operation, the spiker must be fired just before the charging of the PFN capacitor has been completed. For both the resonant overshoot and the charge mode the delay of the spiker thyatron relative to the trigger of the main thyatron had to be adjusted within a window of about 50 ns around the optimum [7].

3. Experimental results

In Fig. 8 we show scans of the output beam in a direction transverse to the electrical field at several values of the PFN-charging voltage and at a purifier temperature of 114 K. The laser operated in the charge mode. It is clear that at low charging voltages, which causes a long delay between gas breakdown and cur-

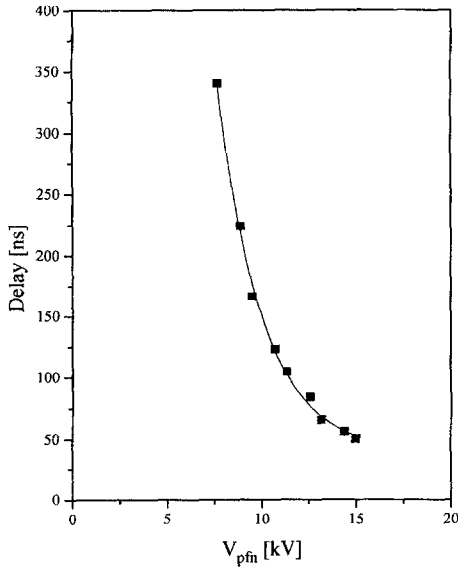


Fig. 6. Delay between the current pulse and the main current pulse as a function of the PFN charging voltage. The laser operates in the charge mode.

rent-rise, a dip in the centre of the laser beam can be observed. This dip can be eliminated by increasing the charging voltage and thus decreasing the delay. The same effect can be obtained by varying the temperature of the purifier. Fig. 9 shows scans at several purifier temperatures at a constant charging voltage of 15 kV. Fig. 10 shows a typical scan for the laser operating in the resonant overshoot mode. A bell-shape profile was observed for all PFN charging voltages and purifier temperatures within the constraints of a stable discharge. This was expected because no delay between the spiker- and the main discharge was present when the laser operated in the resonant overshoot mode.

Following Treshchalov and Peet [3], the modification of the spatial distribution of the discharge can be explained by examining the time- and spatial dependencies of the densities of electrons, $n_e(x, t)$, and vibrational excited HCl ($v > 0$), $[HCl](x, t)$. A simple model consisting of two coupled rate equations illustrates the mechanism:

$$\begin{aligned} \frac{\partial}{\partial t} [HCl](x, t) &= -k_a n_e(x, t) [HCl](x, t), \\ \frac{\partial}{\partial t} n_e(x, t) &= -k_a n_e(x, t) [HCl](x, t), \end{aligned} \quad (1)$$

where $k_a \sim 5 \times 10^{-9} \text{ cm}^3/\text{s}$ [3] is the effective rate of dissociative attachment to HCl ($v > 0$). Choosing an (arbitrary) Gaussian initial distribution for the densities of both the electrons and HCl ($v > 0$) with typical peak values of $n_e(0, 0) = 2 \times 10^{15} \text{ cm}^{-3}$ and $[HCl](0, 0) = 2 \times 10^{16} \text{ cm}^{-3}$ [3] we find that these distributions evolve within a few tens of nanoseconds as shown in

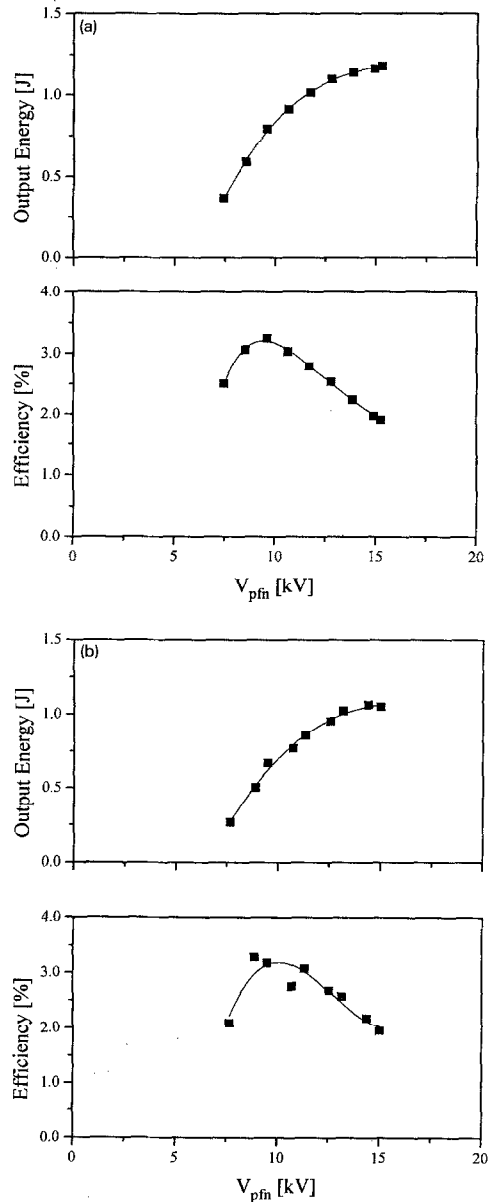


Fig. 7. Laser output energy and efficiency of the laser operating in the resonant overshoot mode (a) and in the charge mode (b).

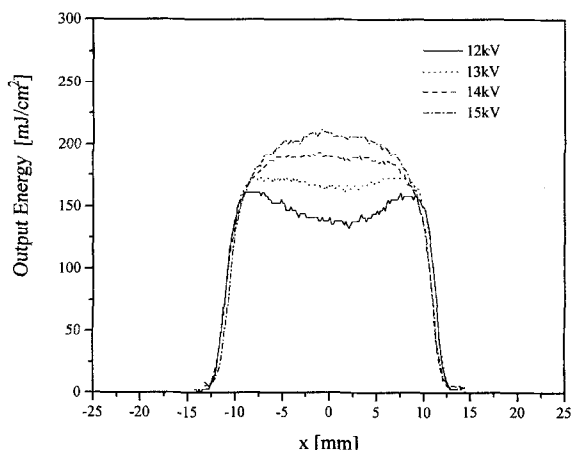


Fig. 8. Scan of the beam profile in the direction transverse to the discharge electrical field where laser operates in the charge mode. Purifier temperature is 114 K ($P_{\text{HCl}}=0.21$ hPa; $P_{\text{Xe}}=3.5$ hPa).

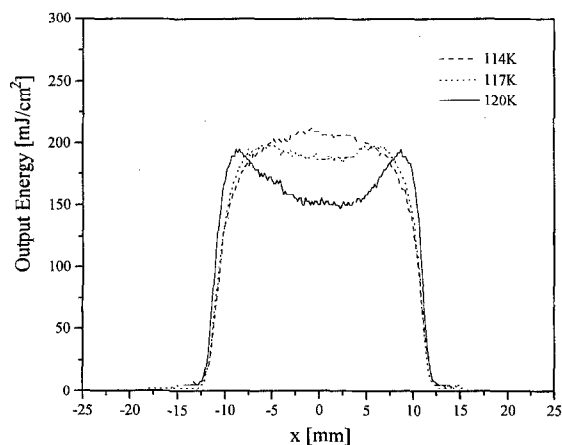


Fig. 9. Scan of the beam profile in the direction transverse to the discharge electrical field where the laser operates in the charge mode. PFN charging voltage is 15 kV. Gas-purifier temperature: 114 K ($P_{\text{HCl}}=0.21$ hPa; $P_{\text{Xe}}=3.5$ hPa), 117 K ($P_{\text{HCl}}=0.34$ hPa; $P_{\text{Xe}}=5.2$ hPa), 120 K ($P_{\text{HCl}}=0.52$ hPa; $P_{\text{Xe}}=7.5$ hPa).

Fig. 11. Decreasing the delay, by raising the PFN charging voltage, results in a less deformed electron density profile yielding a smaller dip in the laser output beam. This is also found experimentally as shown in Fig. 8. An increment of the HCl partial pressure in the gas mixture of a few tens of a hPa increases the initial HCl($\nu > 0$) density slightly. For a given delay between the spiker- and the main pulse the evolution of the electron density profile speeds up, which results in a more pronounced dip in the beam profile. This is in

qualitative agreement with the observations presented in Fig. 9. When the laser operates in the resonant overshoot mode the wave form of the spiker voltage differs from the voltage wave form of the spiker pulse for charge mode operation. For the resonant overshoot mode the voltage changes polarity and the rise time and break down voltage are less compared to those of the charge mode waveform. Because of this the initial values and spatial dependency of several species in the gas discharge will differ for the two modes resulting in a different profile of the initial HCl($\nu > 0$) density. However, this cannot explain the absence and the appear-

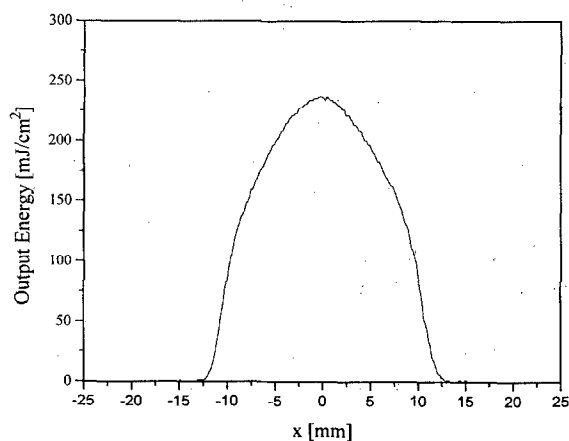


Fig. 10. Scan of the beam profile in the direction transverse to the discharge electrical field where laser operates in the resonant overshoot mode. PFN charging voltage is 15 kV; purifier temperature is 117 K ($P_{\text{HCl}}=0.34$ hPa; $P_{\text{Xe}}=5.2$ hPa).

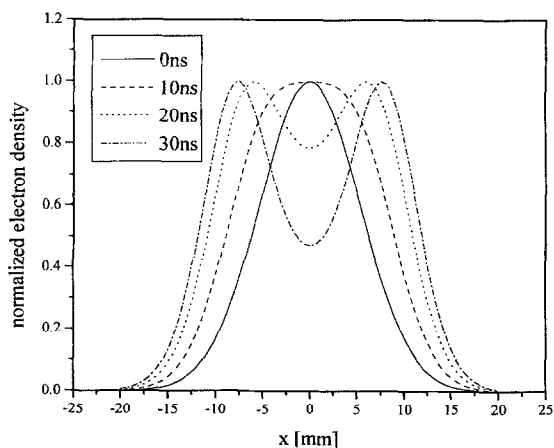


Fig. 11. Calculated spatial and temporal evolution of the electron density in a direction transverse to the discharge electrical field.

ance of the dip in the profile of the beam for the overshoot- and charge mode operation respectively.

4. Conclusions

In conclusion we have demonstrated that the beam profile of a XeCl excimer laser in a direction transverse to the electric field of the discharge can be varied by delaying the main discharge current in respect of the spiker pulse exciting the discharge. This can be done by operating the laser in the charge-mode in which mode the saturation of a saturable inductor in the opposite direction after the initiation of the discharge causes the delay. Modification of the beam-shape can also be obtained by variation of the partial HCl pressure.

The evolution of the beam profile from a “bell-shape”, through a “top-hat” to a “camel-back” profile during the delay has been explained by a spatial redistribution of the electron density caused by dissociative attachment to vibrationally excited HCl. This mechanism can be used to fine-tune the beam profile to the desired shape during operation of the laser. It is expected that this can be applied to a number of applications involving high repetition rate XeCl lasers.

Acknowledgements

The authors would like to acknowledge the support of this research by the Nederlands Centrum voor Laser Research (NCLR). We also want to express our thanks for valuable discussions with Jan van Spijker and Thomas Hofmann from NCLR.

References

- [1] E.A. Petrukhin and A.S. Pososonnyi, *Sov. J. Quantum Electron.* 21 (1991) 269.
- [2] M. Bähr, W. Bötticher and C. Choroba, *IEEE Trans. on Plasma Sc.* 19 (1991) 369.
- [3] A.B. Treshchalov and V.E. Peet, *IEEE J. Quantum Electron.* QE-24 (1988) 169.
- [4] F.A. van Goor, W.J. Witteman, J.C.M. Timmermans, J. van Spijker and J. Couperus, *SPIE Vol. 2206* (1994) 30.
- [5] F.A. van Goor, *J. Appl. Phys. D: Appl. Phys.* 26 (1993) 404.
- [6] J.W. Gerritsen, A.L. Keet, G.J. Ernst and W.J. Witteman, *J. Appl. Phys.* 67 (1990) 3517.
- [7] J.C.M. Timmermans, F.A. van Goor and W.J. Witteman, *Appl. Phys. B* 57 (1993) 441.
- [8] R.S. Taylor, K.E. Leopold and M. von Dadelszen, *SPIE Vol. 2206* (1994) 130;
R.S. Taylor and K.E. Leopold, *Appl. Phys. B* 59 (1994) 479.